Analysis of pillar design practices and techniques for U.S. limestone mines

A.T. Iannacchione

Synopsis

Underground stone mining is an emerging sector of the U.S. mining industry. As this expansion takes mines under deeper cover, and as more efficient mining methods are utilized, effective stone pillar design methods will become even more important. Current design practices are examined and a discussion of safe mine layouts is presented as a first approach towards weighing the demands for increased production against increased risk. Risks to underground stone-mine workers include rib instabilities, pillar failures and roof falls.

Seventy-two stone-mine pillar designs were examined. Pillars with width to height ratios of less than 1.5 appear more likely to fail when subjected to excessive stress levels. When width to height ratios fall below 1.0 defects in the pillars, such as through-running discontinuities, can have a significant influence on stability. Discontinuity persistence, dip, material properties and orientation are also important determining factors in pillar strength.

During the past three years the number of active underground stone mines in the U.S.A. has ranged between 90 and 100. This number is expected to increase as the crushed stone industry responds to growing demands for its products.[1] As more of the industry moves to benefit from the advantages of underground mining production from underground stone mines is expected to increase above its current level of approximately 66 000 000 t/year. Parker[2] identified four advantages of underground mining operations: (1) surface developments, zoning laws and environmental concerns are often less of an issue; (2) stripping and restoration requirements are eliminated; (3) additional reserves are often available beneath the quarry floor, under pit slopes or under an adjoining property; and (4) space is created for secondary use. Underground mines enjoy the added benefits of work in a constant underground climate, rather than in the variable surface climate, minimization of community concerns by placement of the crushing, sizing and stowing operations underground and reduction of surface vibration concerns through smaller blasts. The drawbacks of underground mining include added health and safety hazards for the stone miners, whose health can suffer from increased exposure to falls of ground, airborne contaminants and fog in large underground openings. Injuries from falls of ground in stone mines have occasionally exceeded the incidence rates for other mineral resources mined underground.[3]

Existing underground stone operations, by comparison with stone operations a decade ago, mine more stone at a faster rate and with larger equipment. Because of high demand mines face increased pressure to yield more stone per production blast. A majority of the miners use the V-cut blasting pattern, which limits the depth or pull for each shot to about 4 m. Therefore, to produce more stone, either the mines must work more faces or existing faces must be enlarged.

The enlargement of underground openings poses problems in the maintenance of strata stability. First, the widths of the mine entries partially control the amount of sag or deflection that any given roof beam can withstand before failure. This deflection can take place quickly after an opening is excavated or much later as weathering processes form additional, thinner beams. Because increased deflection increases the potential for roof beam failure, there is a limit to how wide a room can safely be made. These limits depend on local geological and stress conditions and, to some extent, the cost-effectiveness of roof-bolting.

Given these room width limitations, underground stone mines have placed more attention on expansion of production through benching where mining thicknesses permit. The heights of rooms partially control the strength characteristics of adjacent pillars: as the room height increases for a given pillar width the pillar width-to-height ratio (w/h) decreases. In general, stone pillars are very strong, but when the width-to-height ratio diminishes the potential for pillar rib instabilities and pillar failures increases (see Fig. 1).

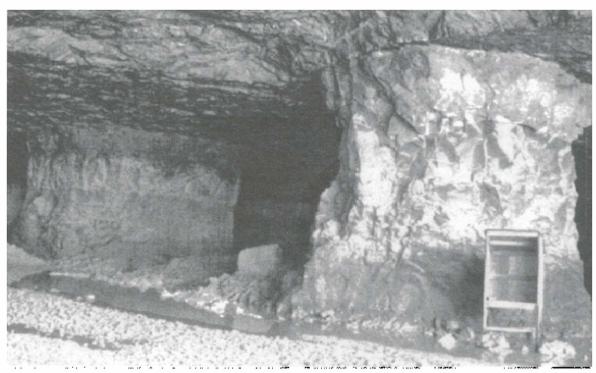

Fig. 1 Concave-shaped failing pillar. Note crushed ribs and slender appearance (w/h <1) of pillar compared with background stable pillar (w/h >1)

In the underground environment the desire to utilize wider rooms, higher benches and multi-level mining results in the potential for unstable ground conditions. Although the number of failed pillars is currently very low, the potential for additional failures will grow if more slender pillars are developed, especially under deeper cover, with wider mining sections and in multi-level operations. It should also be noted that the passage of time acts to decrease the strength of many existing pillars. An examination of current design practices

Manuscript first received by the Institution of Mining and Metallurgy on 12 June, 1999; revised manuscript received on 3 November, 1999. Paper published in *Trans. Instn Min. Metall. (Sect. A: Min. industry)*, 108, September–December 1999.

was undertaken with these trends in mind and the findings are presented here together with a discussion of the principles for safe mine layouts.

Current stone pillar design practices

The National Institute for Occupational Safety and Health (NIOSH) of the U.S.A. surveyed 70 underground stone mines between 1996 and 1998 to collect information on pillar design practices. With one exception every mine used the room-and-pillar mining method. There were, however, some variations in the room-and-pillar method between the mines.

In relatively flat-lying beds the pillars are usually arranged in regular, recurring patterns. Of the 70 mines surveyed, 93% employed regular pillar patterns. Occasionally, random pillar patterns have been used, but this practice has decreased in response to improvements in surveying and mine planning. Currently, only two of the surveyed mines retain the random method.

The majority of mines use square pillars, i.e. whose width is equal to the length. Nine mines use rectangular pillars (hereafter referred to as rib pillars) whose length is greater than their width. Rib pillars have been employed by two prominent consultants in the field, Jim Scott[4] and Jack Parker,[5] for special situations.

The room-and-pillar method takes on some unique characteristics when used in mines with steeply dipping beds with multi-levels. Generally, one to three entries are driven along the strike of the strata, which may dip from 45° to 70°. Crosscuts are developed horizontally, perpendicular to the entries. Raises or windows between the outer, updip crosscuts and the inner, downdip crosscuts provide for ventilation passages between mining levels. Only two of the surveyed mines use this method.

The stoping method, which employs raises, crown pillars, etc., is used by only one mine with steeply dipping beds.

Because 93% of the mines surveyed use the regular room-and-pillar technique in a flat-lying seam, the present study focuses on the analysis of this design method.

In the room-and-pillar method entries and crosscuts are generally driven perpendicular to each other. When these headings are developed horizontally into unmined strata they are called room entries. These rooms outline development pillars. Faces are advanced by the drilling of horizontal holes and blasting of the rock back into the development headings. Seventy-two development mining scenarios (two of the 70 mines surveyed used multiple development designs) with 63 square pillar designs and nine rib pillar designs were examined. The average size of the development pillars was 12.2 m wide × 7 m high (see Table 1). The width of adjacent rooms averaged 13.1 m.

It should be noted that the application of averages from a data-set such as this can produce unsatisfactory results on account of variations in rock mass conditions. For example, a wide range of discontinuity spacing orientation and persistence was observed between field sites; in practice, very small pillars can be stable when discontinuity occurrence is low. Unfortunately, detailed information on the rock mass characteristics was not collected in the present study.

If the stone deposit is thick enough, benching of the floor can occur. Benching can alter slightly the widths of the entries or the pillars. Bench faces are advanced by the drilling of vertical floor holes from development entries and blasting the rock back into the benched headings. Bench heights average 7.6 m. A few of the deeper benches are mined in multiple lifts. More importantly, benching influences the height of the rooms and pillars, which has a direct effect on the pillar width-to-height ratio (see Table 1). Thirty-five of the mines surveyed bench with the room-and-pillar method.

The distribution of width-to-height ratios for all 70 mines surveyed in this study is shown in Fig. 2. Two distinct distributions are observed, reflecting the functional characteristics

Table 1 Mine layout characteristics for underground U.S. stone mines

Characteristic		**Mean**	**Standard deviation**	**Median**	**Minimum**	**Maximum**
Development	Pillar height, m	7	1.7	7	3.7	12.2
	Opening width, m	13.1	2.6	12.8	6.1	18.3
	Pillar width, m	12.2	4.1	12.2	4.6	27.4
	Extraction ratio	0.76	0.07	0.75	0.56	0.91
	Pillar w/h	1.73	0.48	1.72	0.54	3.13
	Overburden, m	80	98	46	7	610
Bench	Pillar height, m	14.6	3.8	14.6	6.7	24.4
	Opening width, m	13.7	2.1	13.7	9.1	18.3
	Pillar width, m	13.1	4.1	13.7	6.1	27.4
	Pillar w/h	0.92	0.35	0.90	0.4	1.92

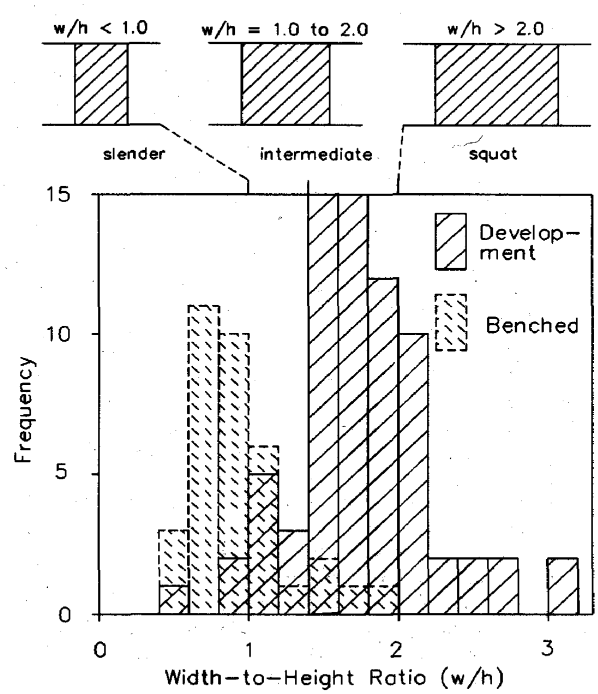

Fig. 2 Width-to-height ratios of pillars used in development and benching sections

of the pillars. The average width-to-height ratio for development pillars was 1.73 with a standard deviation of 0.48, whereas the average ratio for benched pillars was 0.92 with a standard deviation of 0.35. As shown in Fig. 2, the distribution of the 72 development pillar designs is relatively normal, whereas that of the 35 benched pillars is slightly skewed to the left.

Pillar performance issues

The extraction ratio is another geometric and economic factor that affects the relationship between the area of a pillar and the area of the adjacent opening along the horizontal plane. The extraction ratio for perpendicular intersections is determined by the equation:

$$e = \frac{(w+r)\times(l+r) - w\times l}{(w+r)\times(l+r)} \tag{1}$$

where e is extraction ratio, w is pillar width, l is pillar length and r is room width.

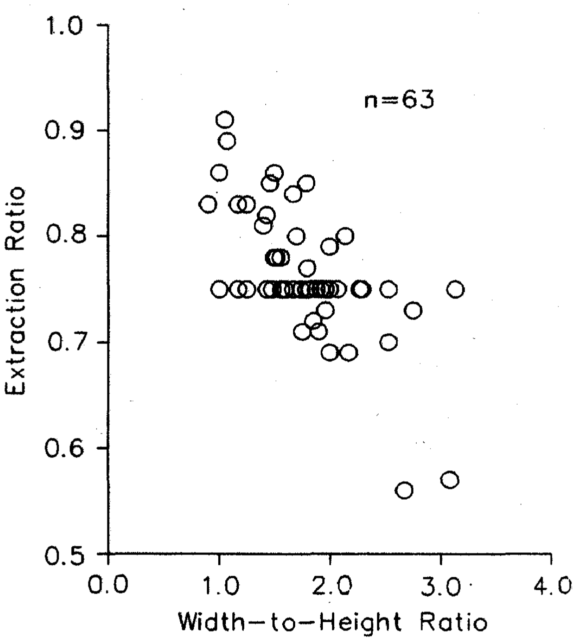

Fig. 3 Comparison between square pillar width-to-height ratios and extraction ratios of development mining

Fig. 3 demonstrates the relationship between the extraction ratio for square development rooms and pillars and the width-to-height ratios for the same pillars. In general, the extraction ratio is decreased as the width-to-height ratio is increased. This is expected because pillar width is a factor considered in both ratios. The safety concern is that as the extraction ratio is increased the pillars become more slender and must support higher levels of stress.

Depending on the number of years over which it has been mined, an underground stone mine may have a few dozen to several thousand pillars. The vast majority of these pillars are adequately sized and currently stable. Pillar design is, however, seldom addressed explicitly in planning. Pillar stability should be more closely examined under (1) excessive stress levels, (2) adverse geological conditions and (3) increasing time.

Stress levels

Generally, stone pillars are expected to be less stable if the overburden is substantial because of the higher stress. Pillars might also be less stable as the width-to-height ratio is decreased, as in benching operations. Stress levels in pillars can be approximated by use of the tributary area theory:[6]

$$\sigma_a = \sigma_o \times \frac{(r+w)\times(r+l)}{w\times l} \tag{2}$$

where σ_a is average post-mining vertical stress and σ_o is pre-mining vertical stress.

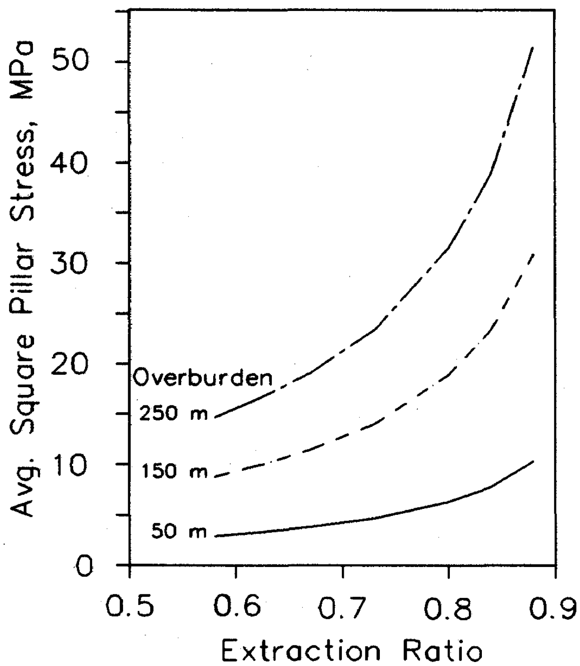

Fig. 4 Relationship between average pillar stress levels, extraction ratios and overburden for 13.7 m wide opening with square pillars

Pillar stress levels are affected, in part, by the overburden and the relationship between the area supported by the pillar and the area of the pillar. This relationship can be illustrated by comparing the post-mining vertical stress levels as the overburden and the extraction ratio increase. Fig. 4 shows the relationship between average pillar stress, overburden and extraction ratio for a 13.7 m wide opening with square pillars. As the overburden and extraction ratios increase the stress levels rise exponentially. Incremental changes in overburden result in a parallel change in the average pillar stress levels at specific extraction ratios. Likewise, increased extraction ratios produce an exponential rise in the average pillar stress levels at specific overburdens. The average overburden for most underground stone mines is 80 m, so excessive stress levels would not be expected to be the cause of pillar failure. The relatively shallow depth of most underground stone mines has historically been the reason why pillar shape and size are often overlooked as a safety issue during mine design and development.

Pillar strength

The most generally accepted techniques for estimating pillar strength, defined as the ultimate load per unit area of a pillar, use empirical derivations based on survey data from actual mining conditions. The strength of the empirical method is that specific failure mechanisms need not be considered. The limitations of the empirical method stem from the inability to extend the formulae beyond the specific material properties, sizes, shapes and overburdens found in the survey data. Bieniawski[7] wrote that the strength of mine pillars is dependent on three elements: (1) the size or volume effect (strength reduction from a small laboratory specimen of rock to full-size mine pillars); (2) the effect of pillar geometry (shape effect); and (3) the properties of the pillar material. For non-coal pillars empirical formulae have largely been derived from some form of the following power formula:[8]

$$\sigma_p = \sigma_m \times \frac{w^a}{h^b} \tag{3}$$

where σ_p is pillar strength (ultimate), σ_m is material strength, h is pillar height and a and b are constants derived from laboratory or field experiments. This formula takes account of both material strength and pillar shape to calculate pillar strength.

Material strength

In these equations the material strength, σ_m, of a nominal size of pillar is generally approximated by reducing the uniaxial compressive strength, σ_c, of the material from laboratory testing of small cylindrical or cubic specimens. Laboratory test samples typically overestimate rock material strength values because larger flaws or fractures are exhibited as the specimen size increases. At some point the specimen size becomes sufficiently large that further reductions in material strength are insignificant. The point at which this occurs is often referred to as 'rock mass strength'. Bieniawski[7] suggested that cubic coal specimens of side 0.9–1.5 m are of a critical size and are representative of rock mass characteristics. Hedley and Grant[9] used an equivalent material strength value representative of a 0.3-m cube of quartzite. Others have used reduction factors that range from 40 to 80% to determine material strength from uniaxial compressive strength values.

Pillar shape

Several pillar strength equations have been expressed as a power function of the pillar's height and width. Equation 4 was derived by Salamon and Munro[10] after analysis of 125 case studies from South African coal mines:

$$\sigma_p = 1320 \times \frac{w^{0.46}}{h^{0.66}} \ (\text{lb/in}^2) \tag{4}$$

In this equation a material strength, σ_m, equivalent to 7.2 MPa, was used because coal has a low material strength by comparison with most industrial minerals and metal-mine rocks. Hedley and Grant[9] extended this power function to describe the strength of quartzite pillars in deep uranium mines near Elliot Lake, Canada:

$$\sigma_p = 26\,000 \times \frac{w^{0.5}}{h^{0.75}} \ (\text{lb/in}^2) \tag{5}$$

This equation is similar to Salamon and Munro's apart from the much higher material strength value for the stiff uranium host rock. In this case the material strength of the uranium pillars is close to 20 times greater than that of South African coal.

An alternative application of a pillar strength formula was suggested by Hardy and Agapito.[11] From a study of western Colorado oil-shale pillars in which discontinuities are closely spaced the appropriate pillar strength formula was inferred to be of the form

$$\sigma_p = \sigma_c \times \left(\frac{v_p}{v_s}\right)^{-0.118} \times \left(\frac{\frac{w_p}{h_p}}{\frac{w_s}{h_s}}\right)^{0.833} \tag{6}$$

where σ_c is uniaxial compressive strength of a sample and v is volume of the pillar/sample. This method involves determination of the uniaxial compressive strength of a specimen and the subscripts p and s refer to the pillar and specimen, respectively.

Power functions produce a very distinctive relationship between strength and the width-to-height ratio (see Fig. 5). At low width-to-height ratios (<1.0) pillar strength rises rapidly. At higher width-to-height ratios increases in strength occur at diminishing rates. In other words, at some point the pillar is believed to display some plastic behaviour. Barron referred to this as pseudo-ductile behaviour.[12] The occurrence of pseudo-ductility in coal pillars has been debated for years. It seems unlikely that stiff, brittle materials, such as stone or other hard rocks, would display the same type of plastic behaviour. In fact, some authors have argued that at width-to-height ratios greater than 4 or 5 strain-hardening behaviour can occur[13,14] because stress distributions and confinement conditions change.

Stacey and Page[14] took this behaviour into account by generating exponential rises in pillar strength at higher width-to-height ratios:

$$\sigma_p = k \times \frac{w^{0.5}}{h^{0.7}} \ (\text{MPa}) \tag{7}$$

for w/h <4.5 and

$$\sigma_p = k \times \frac{2.5}{V^{0.07}} \times \left\{ 0.13 \times \left(\left[\frac{\left(\frac{w_{\text{eff}}}{h}\right)}{4.5} \right]^{4.5} - 1 \right) + 1 \right\} \ (\text{MPa}) \tag{8}$$

for w/h >4.5

where $k = \sigma_m \times$ DRMS, Design Rock Mass Strength[14] (DRMS) being the σ_c adjustment factor; and $V = w^2_{\text{eff}} \times h$, w_{eff} being equal to $4 \times A_p/R$ where A_p is plan area of the pillar and R is its perimeter. Here the pillar strength follows a power function for a relatively low width-to-height ratio (<4.5) and thereafter begins an exponential rise (see Fig. 5). The pillar strength formula for w/h >4.5 was taken almost directly from the Salamon–Wagner squat pillar strength formula published a year earlier. Stacey and Page's formula is used from here on because it was developed for hard rocks.

The application of these formulae to underground stone is problematic. It seems unlikely that increasing the pillar width-to-height ratio would result in a gradual decrease in the rise in pillar strength. In fact, in practice just the opposite appears to occur. Pillar stability is jeopardized most at low width-to-height ratios. As typical stone pillars reach a width-to-height ratio >1.5 they begin to exhibit an almost indestructible character in shallow mines. Nevertheless, the Stacey and Page[14] formula appears to accommodate both the traditional strength flattening at moderate width-to-height ratios (*ca* 4–5) proposed by Salamon and Munro[13] and the exponential rise in pillar strength at high width-to-height ratios. Unfortunately, this strength adjustment occurs at width-to-height ratios that are well outside the ranges of the stone mines surveyed.

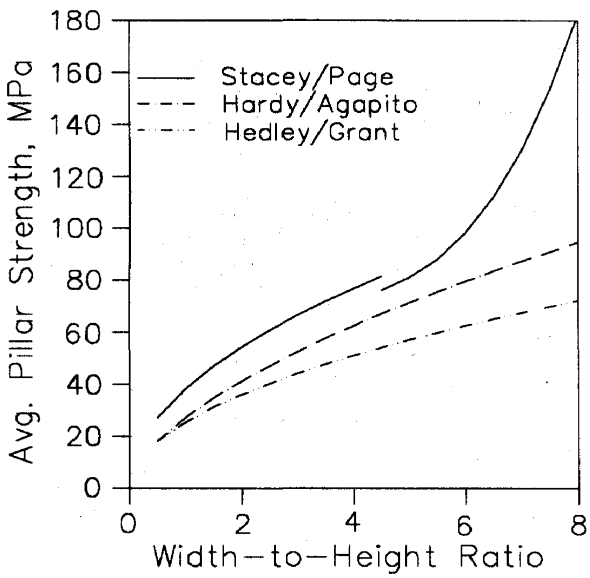

Fig. 5 Comparison between pillar width-to-height ratio and average pillar strength for different empirical equations based on power function.[9,11,14] Material strength was normalized for each equation for comparative purposes

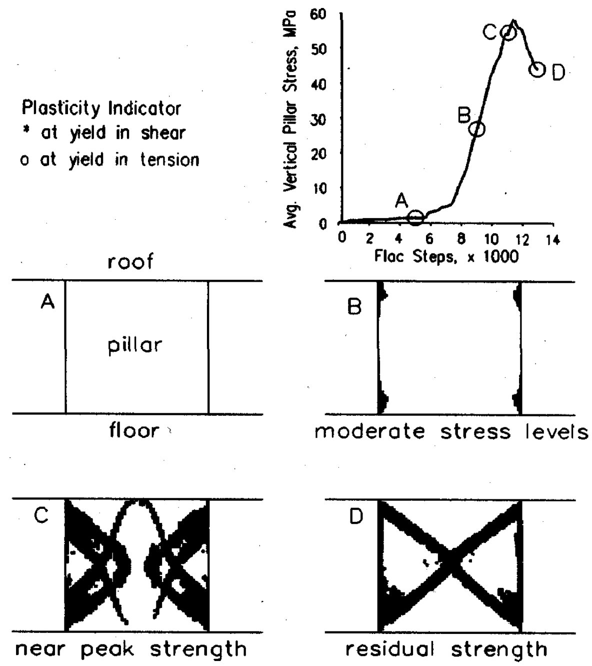

Fig. 6 Elastic–plastic model, which produces progessive failure patterns, can demonstrate strain-softening behaviour within full-scale pillars

Progressive failure in stone pillars

Owing to the limitations of survey data, the above empirical methods do not provide a totally realistic picture of stone pillar behaviour. Additionally, a large database of pillar-specific information that represents past successes and failures has not been established to aid in construction of a reliable pillar design technique for stone mines. In the absence of this information numerical simulations can provide a potentially useful means of testing engineering methods.

The simulation used for this study was the two- and three-dimensional finite-difference code.[15] The two-dimensional calculations were performed under plane-strain conditions, so the model sample is equivalent to a long pillar. It was assumed that individual elements in the model behaved in an elastic–perfectly plastic manner; the overall pillar behaviour could, however, include strain softening and strain hardening. Model shapes mirrored those observed in the field and ranged from a very slender pillar with a width-to-height ratio of 0.4 to intermediate pillars with a width-to-height ratio of 1.4. Model symmetry was constructed to simulate a recurring pattern of rooms and pillars of equal dimensions. The roof and floor materials were modelled to be elastic.

Slender-shaped pillars failed rapidly by yielding from the ribs inwards to the pillar core, which indicated a relatively low-strength structure. As the pillars became more squat, elevated horizontal confinement increased their strength greatly.

The model pillars had a modulus of 41.4 GPa, an angle of internal friction of 40° and a cohesion of 6.9 MPa. These data were derived from laboratory tests of the Layolhanna Limestone in Pennsylvania. The model pillars were subjected to simulated loading conditions by moving distant boundaries in the roof and floor together at very slow rates. This had the effect of a gradual loading of the pillars through several distinct strength phases. During the early loading phase the modelled pillar displayed relatively elastic characteristics (Fig. 6, points *A*–*B*), the deformation of the pillar being proportional to increases in average vertical stress levels within it.

During this phase dominated by elastic behaviour minor yielding of the pillar edges began to occur. Continued progressive failure of the pillar's outer perimeter produced an hourglass-shaped elastic core. It also had the effect of moving the peak vertical stress away from the pillar edge towards the pillar centre (Fig. 6, points *B*–*C*).

The maximum pillar strength was achieved when the highest vertical stress levels in the elastic core were supported by the maximum horizontal confinement available to the pillar (Fig. 6, point *C*). Beyond this point any additional load to the pillar resulted in rapid loss of strength. The zone of plastic yield extended throughout the pillar, producing a residual pillar strength (Fig. 6, point *D*) that was considerably less than the maximum pillar strength.

Effect of excessive stress on stone pillar stability

Pillar failure due to excessive stress levels was not frequently observed during field visits to these mines. In fact, only seven development pillars at four mines were observed to have undergone progressive failure due to excessive loading (Table 2). In case 1 (Table 2), a pillar with a width-to-height ratio of 1.0 was inadvertently reduced from 9.1 to 6.1 m under less than 30 m of overburden. The calculated average vertical stress for this pillar was less than 7 MPa: in reality, the stress levels may have been much higher. Failure of the pillar perimeter due to crushing left only a narrow core of broken rock (Fig. 1). It was surmised that additional stresses were applied to the pillar either as a consequence of its unique position near the highwall and the effect of some undetected geological characteristic or by deflection of the roof in overwide openings.

In case 2 the initial mine development had taken place by random room-and-pillar methods. One failed pillar was observed to be narrower than the surrounding pillars. This

Table 2 Characteristics of development pillars that failed

Case	Observed failed pillars	Pillar width, m	Pillar height, m	Ratio *w/h*	Extraction ratio	Reason for failure
1	1	6.1	6.1	1.0	0.94	Reduced pillar size
2	1	6.1	4.9	1.25	0.92	Smallest pillar in non-regular mining area
3	1	5.5	6.1	0.9	0.86	High overburden stress and reduced pillar size
4	4	3–6.1	7.3	0.42–0.83	0.9–0.83	High overburden stress

pillar had a width-to-height ratio of 1.25, whereas adjacent pillars were in excess of 2.0. Here again it was difficult to determine what level of stresses had caused failure because the overburden was very low.

In case 3 a pillar with a width-to-height ratio of 0.9 was inadvertently reduced from 9.1 to 5.5 m under a high overburden condition of approximately 275 m. Average vertical stresses on this pillar could have exceeded 28 MPa. The failed pillars had shear surfaces that began and terminated at the pillar–roof and pillar–floor intersections and propagated inward in a convex shape (Fig. 1).

In case 4 the overburden ranged from 230 to 260 m and produced an average vertical stress that was generally less than 14 MPa on pillars with openings that ranged between 15 and 18 m in width and with width-to-height ratios that averaged 2.1. In several areas within this large mine pillars of reduced width with width-to-height ratios ranging from 0.83 to 0.42 were subjected to average vertical stresses that could have reached 35 MPa. At least four of these pillars exhibited a very distinctive concave failure surface that resembled an onion skin. As the failure process continued the pillar size was reduced, thereby increasing the extraction ratio and resulting in higher stress and more pillar deterioration.

Pillar design guidelines

As underground stone production expands mining depths (overburden) are expected to increase. At present, six mines in the Valley and Ridge Province of Pennsylvania, Virginia and Tennessee and two mines in Kentucky are worked at depths between 250 and 600 m. Many more mines will soon encounter their first 100–150 m overburdens. As the depth of mining is increased the potential for excessive stress levels that affect pillar stability adversely will also increase.

In the absence of well-established design information for underground stone mines pillar design guidelines related to excessive stress levels are proposed. These guidelines make use of the previous numerical simulations as a means of examining how pillars of various shapes will be affected under different overburdens. Fig. 7 shows changes in average vertical stress conditions at different overburdens and different width-to-height ratios based on the tributary area theory. The solid black lines represent the strength of a modelled pillar, free of discontinuities, as its shape is changed from a slender pillar (*w/h* = 0.4) to an intermediate pillar (*w/h* = 1.4). This modelled pillar has a stiffness of 41.4 GPa and a failure envelope defined by a friction angle, ϕ, of 40° and a cohesion of 6.9 MPa. These values represent typical material strength characteristics of the Loyalhanna Limestone of Pennsylvania and West Virginia, which is a relatively high-silica limestone (10–40%) with extensive cross-bed structures.

In this example the modelled pillar with a width-to-height ratio of 1.4 could accommodate an average vertical stress of approximately 80 MPa. Clearly, a pillar of this strength, free of discontinuities, could withstand all of the extraction ratio and overburden conditions set forth in Fig. 4. Conversely, a slender pillar, with a width-to-height ratio of 0.6 and 250 m of overburden, might fail.

The FLAC model strength curve (Fig. 7) has a shape very different from that of curves determined by the empirical design techniques illustrated in Fig. 5. At low width-to-height ratios pillars are low in strength. As width-to-height ratios increase to 1.0 and beyond the pillar strength is increased considerably. At a width-to-height ratio of greater than 1.5

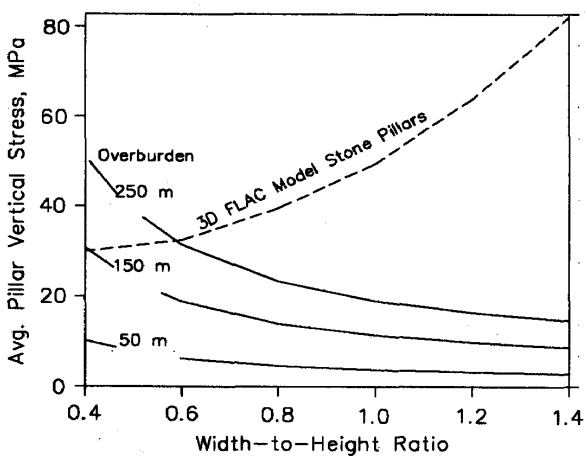

Fig. 7 Changes in stone pillar strength at width-to-height ratios ranging from 0.4 to 1.4

pillars that are free of geological discontinuities are unlikely to fail. The shape of the pillar strength curve shown in Fig. 7 is defined by the stiffness of the material and shape of the failure envelope, which is defined by the friction angle and the material cohesion used in the model.

Effect of discontinuities on stone pillar stability

The stability of a stone pillar can be influenced greatly by overburden stresses and the occurrence of geological discontinuities. Observations of pillar conditions have shown that the presence of geological discontinuities is more likely to represent a threat to workers' safety than excessive stress levels. When the height of a room is increased the area of the rib is increased, which exposes more geological discontinuities and creates more potential for mining-induced damage to intersect the rib. Mining-induced damage can result from drilling, blasting or scaling operations and is an extremely important factor for the design of safe, stable pillars, although it is not considered in detail here. Blast damage, for example, can extend as much as 30 diameters from ANFO-filled blastholes (i.e. 1–2 m into the pillar), thus taking 2–4 m off the dimensions of a square pillar.

Bench mining case studies

The best way to analyse the influence of geological discontinuities on pillar stability is to evaluate pillar performance in benching operations, where pillar shapes are generally slender. A comparison of pillar shape, room width and pillar height of 35 square bench pillar designs is shown in Fig. 8.

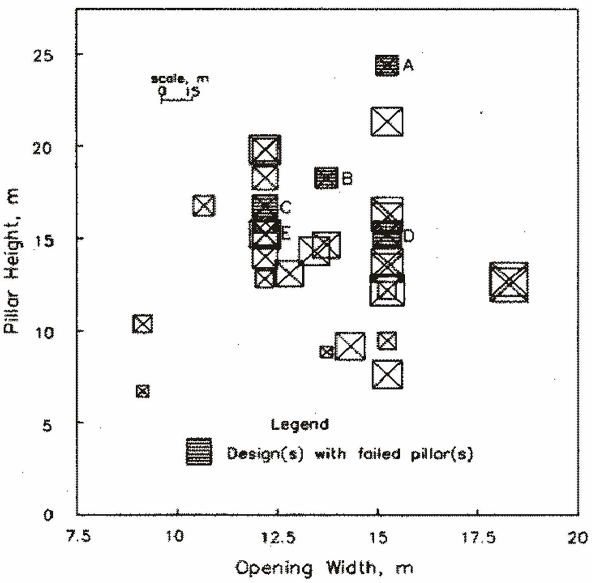

Fig. 8 Comparison of pillar shape, opening width and pillar height of 35 square bench pillar designs. Changes in square size are proportional to changes in pillar sizes

There appears to be no clear correlation between pillar height or room width and pillar failure. Indeed, three of the four designs with some failed pillars had only moderate pillar widths and heights (Fig. 8, points *B*, *C* and *D*). These operations were all mining in a formation that is known to have a higher than normal occurrence of large, high-angle geological discontinuities. The fourth design with failed pillars (Fig. 8, point *A*) was used in a formation that is not known to have a high occurrence of geological discontinuities; failure here was probably associated with the slenderness of the pillar ($w/h = 0.5$).

Several characteristics determine the significance of a geological discontinuity: (1) *persistence*—the length of a discontinuity must be on the same scale as the pillar itself if its strength is to be seriously impaired; (2) *dip*—the dip of a discontinuity can affect pillar strength dramatically (Fig. 9); (3) *frequency*—the spacing between discontinuities is very important in determination of the potential for failure in a large mining area; (4) *material properties*—the properties of a discontinuity can be used to assess the magnitude of strength reduction; and (5) *orientation*—the orientation of a discontinuity is important when the pillars are rectangular in that strength will be affected most if the discontinuity is aligned with the long axis of the pillar.

Fig. 9 Left pillar has multiple sets of discontinuities that dip at 50–70°; right pillar has two prominent discontinuities that dip at approximately 60°

Characteristics of discontinuities

Several of the factors outlined above can be considered by use of the analytical procedure discussed by Farmer:[16]

$$\sigma_1 = \frac{2C_d + 2\sigma_3 \tan\phi_d}{(1 - \cot\beta \tan\phi_d)\sin 2\beta} \tag{9}$$

where σ_1 is vertical strength, σ_3 is confinement, C_d is cohesion along the discontinuity, ϕ_d is friction angle along the discontinuity and β is dip of the discontinuity measured from the vertical axis.

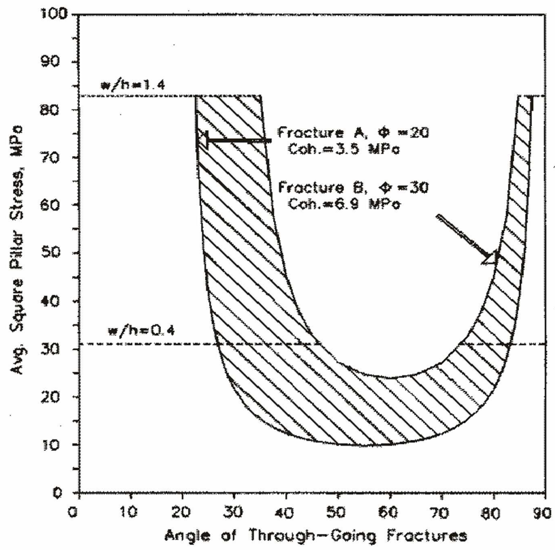

Fig. 10 Effect of angular geological discontinuities on vertical strength by use of analytical technique

Fig. 10 shows how sample strength varies with discontinuity dip angles for different discontinuity material properties. This analysis not only demonstrates the relative magnitude of strength reduction based on discontinuity dip angle but it also shows how friction angle and cohesion along the discontinuity individually affect unit strength. However, the value of this technique in the analysis of stone pillar behaviour with discontinuities is limited because it treats the material as one uniform elastic mass.

An alternative approach is to introduce simulated discontinuities into the previously discussed finite-difference elastic–plastic pillar model and rotate the interface through a series of angles. In this way variations in material properties, discontinuity dips and pillar shapes can be evaluated. This was accomplished by use of the ubiquitous-joint model in the FLAC 3D program. The ubiquitous-joint model is an anisotropic plasticity model that includes weak planes of specific orientation embedded in a Mohr–Coulomb solid. In this model yielding may occur either in the intact rock or along a joint (discontinuity) or both, depending on the stress state, the orientation of the joint plane and the material properties of the intact rock and joint plane.

Parametric analysis of the effect of discontinuities on pillar strength was conducted by varying the dip and material properties within the ubiquitous-joint model. In these simulations discontinuities were passed through modelled pillar shapes whose width-to-height ratios ranged from 0.6 to 1.2. Three distinct pillar behaviours were observed in relation to the dip of the discontinuities. Fig. 11 shows the strength profiles for

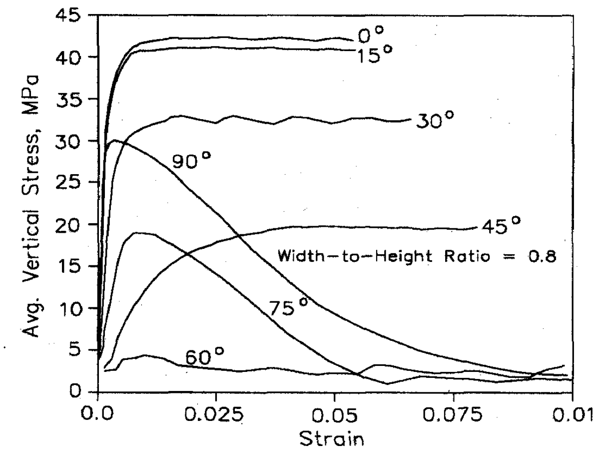

Fig. 11 Stress versus strain for model pillars (width-to-height ratio = 0.8) with discontinuity dips ranging from 0 to 90°

pillars with a stiffness of 41.4 GPa and a Mohr–Coulomb failure envelope defined by a friction angle of 40° and a discontinuity friction angle of 25°. The lowest pillar strength occurred at a discontinuity dip angle of 57.5° (Fig. 11). It should be noted that the point of lowest strength is defined in the ubiquitous-joint model by the relationship

$$\beta_{min} = 45 + \frac{\phi_d}{2} \tag{10}$$

where β_{min} is the angle of a through-running discontinuity that produces the lowest average vertical peak stress and ϕ_d is the internal angle of friction of the discontinuity.

How well this model characteristic fits field conditions needs further evaluation. The highest pillar strength occurred with a discontinuity dip of 0° and gradually decreased as the dip angle increased. As the discontinuity dip angle increased above 57.5°, however, the pillar strength began to increase again, but the original strength for the intermediate to squat pillar shapes was not re-established as failure shifts to a different mode.

For all model shapes and for a given set of material properties the pillar strength associated with a discontinuity dip of 90° was the same. In the case shown in Fig. 11 that value was approximately 29 MPa. This characteristic may, however, be model-driven and not representative of field conditions. The ubiquitous-joint model attempts to force discontinuities through columns of grid elements of equal size. Although this behaviour may be indicative of successive column failure through a pillar with numerous, equally spaced vertical joints, it may not be indicative of pillars affected by variably spaced joints.

Stress versus strain plots for these numerical simulations are shown in Fig. 11. For discontinuity dips between 0 and 45° the material displayed elastic–plastic behaviour. When the model was run with a discontinuity dip of 60° the model pillar exhibited very low strength. Finally, strain-softening material behaviour occurred as the discontinuity dips increased to 90°. Thus, both observation and numerical data suggest that when discontinuities are present at a particular angle and composition they can control the behaviour and strength of pillars.

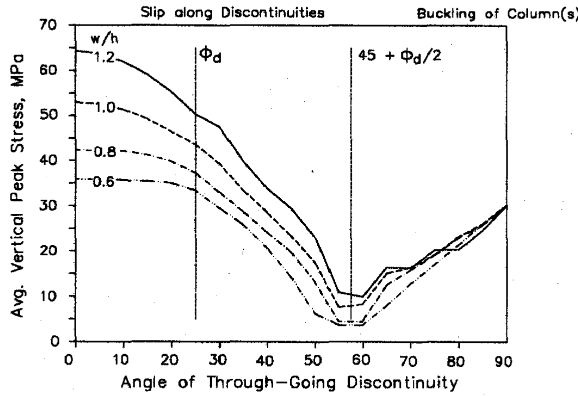

Fig. 12 Changes in vertical peak stress as discontinuity dips are varied from 0 to 90° for four different width-to-height ratio model pillars

The implications of this analysis are revealed in Fig. 12. As demonstrated, the strength of pillars of various shapes and with different discontinuity dips is very sensitive to changes in extraction ratio and overburden. For example, a discontinuity dipping at 60°, under approximately 50 m of overburden, with a width-to-height ratio of 0.8 and passing through the entire 15 m high pillar, could cause failure if its properties were equivalent those of material with a friction angle of 25° and a cohesion of zero. If this same discontinuity dips at 45°, the pillar might not fail until almost 250 m of overburden is encountered. Fig. 13 is presented to illustrate the significant impact that pillar shape, overburden and discontinuities can have on stone pillar strength, but it is not meant to be a design guideline.

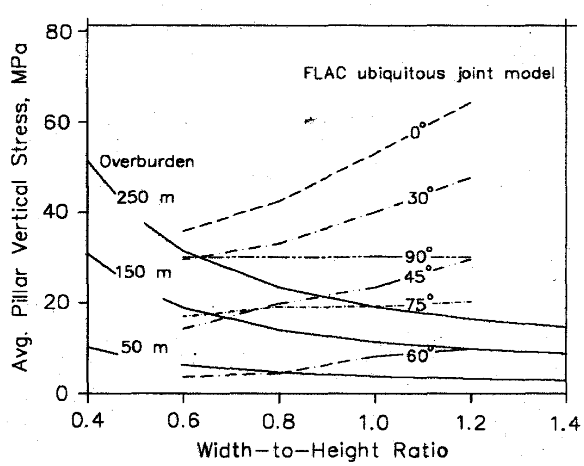

Fig. 13 Relationship between pillar shape, overburden, discontinuity dip and pillar stress

Summary and conclusions

The aim of the present report is to enhance mine-worker safety by increasing awareness of the potential for pillar failure—in particular, in operations that bench. As underground stone mining expands and the depth of overburden is increased consideration of the appropriate size and shape of pillars should be an integral part of overall mine design. Data gathered from mine visits, mine maps, discussions with operators and numerical simulations have been applied in an investigation of stone pillar design issues and general guidelines have been discussed.

The important pillar design issues and guidelines can be summarized as follows.

(1) Most stone pillars have relatively low width-to-height ratios, ranging from 0.54 to 3.13, and high extraction ratios, ranging from 0.56 to 0.91. This results in many pillars having slender shapes with relatively large adjacent mine openings.

(2) Excessive vertical stress levels are generally not a serious problem in stone mines because the pillar material is often very strong and the overburdens are typically very low (the average overburden is 80 m). A few cases are known, however, in which pillars have failed due to excessive local stress levels. These failures were associated with local, unintentional pillar size reduction, overburdens greater than 200 m, width-to-height ratios less than 1.25 or extraction ratios greater than 0.83. As the depth of mining increases the potential for excessive stress levels that affect pillar stability adversely will also increase substantially.

(3) The strength of slender pillars is best understood by examining models that allow for shape variations and progressive failure through elastic–plastic or strain-softening behaviour. Models that meet these criteria have demonstrated that stone pillar strength should not follow a straight linear relationship with pillar shape. Empirical strength formulae for metal and non-metal mines yield power curves that produce higher pillar strengths at low width-to-height ratios (<1.0) and lower pillar strengths at moderate to high width-to-height ratios (>1.5).

(4) Bench mining produces slender pillars. Where geological discontinuities are present the potential for pillar failures increases. The persistence, dip, frequency and material properties of these discontinuities control pillar strength.

(5) A strong correlation was found between the material properties and dip of discontinuities and the modelled pillar strength. As discontinuity dips increased from 0 to $45° + \phi_d/2$ pillar strength gradually decreased. When the dips were equal to $45° + \phi_d/2$ pillars exhibited a very unstable behaviour with the loss of considerable amounts of their original strength. As vertical orientations were approached columns defined by discontinuities could have controlled pillar behaviour.

The pillar design guidelines developed through the observational and numerical simulations discussed above require further field confirmation. The information has been presented so that mine planners, operators and workers can recognize the potential hazards that exist when designing stone pillars. This approach can help to form part of a comprehensive, proactive, ground-control plan to improve safety in underground stone mines.

References

1. Anon. Highway-building surge. *Wall Street J.*, June 2, 1998, A1(W)–A1(E).
2. Parker J. Everybody goes underground eventually. *Aggregate Manager*, June 1996, 30–5.
3. Iannacchione A. T., Mucho T. P. and Prosser L. J. Ground control problems in the underground limestone industry. In *Proc. Environment, safety and health forum (National Stone Assoc.), Nashville, TN, Oct. 22–24, 1995.*
4. Iannacchione A. T. and Prosser L. J. Roof and rib hazard assessment for underground stone mines. Presented at SME Annual meeting, Denver, CO, Feb. 24–27, 1997. SME Preprint 97-113, 5 p.
5. Parker J. How to design better mine openings: practical rock mechanics for miners. *Engng Min. J.*, 174, December 1973, 76–80.
6. Brady B. H. G. and Brown E. T. *Rock mechanics for underground mining* (London: George Allen and Unwin, 1985), 320–5.
7. Bieniawski Z. T. *Rock mechanics design in mining and tunneling* (Rotterdam: Balkema, 1984), 193–209.
8. Agapito J. F. T. Pillar stability in large underground openings: applications from a case study in competent, jointed rock. *Colorado School of Mines Q.*, 8, no. 3, 1986, 52 p.
9. Hedley D. G. F. and Grant F. Stope-and-pillar design for the Elliot Lake uranium mines. *CIM Trans.*, 75, 1972, 121–8.
10. Salamon M. D. G. and Munro A. H. A study of the strength of coal pillars. *J. S. Afr. Inst. Min. Metall.*, 68, 1967, 55–67.
11. Hardy M. P. and Agapito J. F. T. Pillar design in underground oil shale mines. In Fairhurst C. and Crouch S. L. eds *Design methods in rock mechanics, Proc. 16th Symposium on rock mechanics Minneapolis, MN, 1975*, 257–66.
12. Barron K. An analytical approach to the design of coal pillars. *CIM Bull.*, 77, no. 868, 1984, 37–44.
13. Salamon M. D. G. and Wagner H. Practical experience in the design of coal pillars. In *Proc. 21st Int. conf. of.safety in mines research institutes, Sydney, Australia, 1985*, 3–10.
14. Stacey T. R. and Page C. H. *Practical handbook for underground rock mechanics* (Trans Tech Publications, 1986), 53–63. *Series on rock and soil mechanics* 12
15. Itasca. *FLAC: Fast Lagrangian Analysis of Continua user's guide* (Minneapolis: Itasca Consulting Group, Inc., 1998).
16. Farmer I. W. *Engineering behaviour of rocks* (London: Chapman and Hall, 1983), 151–8.

Author

Anthony T. Iannacchione, who holds a Ph.D. in civil engineering from the University of Pittsburgh and is registered as a professional engineer and geologist in Pennsylvania, U.S.A., is Deputy Director of the Pittsburgh Research Laboratory of the National Institute for Occupational Safety and Health (NIOSH).

Address: National Institute for Occupational Safety and Health, Pittsburgh Research Laboratory, P.O. Box 18070, Pittsburgh, PA 15236-0070, U.S.A.